THE
PHYSICAL REVIEW

*A journal of experimental and theoretical physics established by E. L. Nichols in 1893*

SECOND SERIES, VOL. 90, NO. 2 APRIL 15, 1953

# Cross Sections for the Formation of the Compound Nucleus by Charged Particles*

MATHEW M. SHAPIRO†
*Physics Department, Massachusetts Institute of Technology, Cambridge, Massachusetts*
(Received January 6, 1953)

Schematic theory is employed to calculate $\sigma_c$, the cross section for the formation of the compound nucleus when the incident particle is a proton, deuteron, or alpha-particle. The results are compared with the measured $(p,n)$, $(\alpha;n,2n,\cdots)$ cross sections. These should agree in the medium energy region where there is little competition to neutron emission. The curves for the theoretical cross sections as a function of energy have the same shape as the experimental curves. In many cases the magnitude of the measured cross sections of different isotopes of the same element differ from one another, and hence from schematic theory results, by about a factor of two.

Tables based on accurate values of the Coulomb wave functions are given for computing the cross section for formation of the compound nucleus by bombardment with protons and deuterons when the atomic number of the target nucleus exceeds 10, and with alpha-particles when the atomic number of the target nucleus lies between 10 and 30. The tables are applicable over a wide range of nuclear radii.

## 1. INTRODUCTION

FESHBACH and Weisskopf[1] have described a theory of nuclear reactions which, on the basis of a very rough picture of nuclear structure, describes the magnitude and energy dependence of nuclear cross sections. In that paper the theory was applied to the calculation of the total cross section, the reaction cross section, and the transport cross section when the incident particle was a neutron.

In the present paper we apply the schematic theory to the calculation of the cross section for the formation of the compound nucleus $\sigma_c$ when the incident particle is charged, in particular, when it is a proton, deuteron, or alpha-particle. The theory treats these particles as indivisible entities. Consequently, the cross sections calculated below do not include the deuteron stripping process.

As before, the theory is to be considered approximate in the sense that it does not reproduce individual fluctuations or resonances. If the latter occur, the results are to be considered as average values over a region containing many resonances. For sufficiently high energies the resonance levels become broader, and finally the dependence of the cross section on energy is represented by a smooth curve. In this region our theoretical predictions are expected to be valid without any averaging.

The theory is based upon a very simplified picture of nuclear structure. In fact, the only information employed about the internal structure of the nucleus is the radius $R$ and the wave number $K$ of the incident particle within the nucleus. The wave number $K$ is estimated by assuming that inside the nucleus in the vicinity of the nuclear surface, the dependence of the wave function on the radial coordinate of the incident particle is periodic with a wave number corresponding to its kinetic energy within the nucleus. It follows that $K^2=K_0^2+k^2$, where $k^2=2M\epsilon\hbar^{-2}$, $M$ is the reduced mass of the particle, $\epsilon$ its kinetic energy in the center of mass system at a point infinitely far from the nucleus, and $K_0$ is the wave number $K$ for zero incident energy. $K_0$ can be estimated by computing the maximum allowed momentum of a Fermi-Dirac particle restricted to the volume $V$.[2] The result is

$$K_0^2=(4\pi)^2(3A/16\pi V)^{\frac{2}{3}},$$

where $A$ is the nuclear mass number and $V$ is the

* This work was supported in part by the U. S. Atomic Energy Commission and the U. S. Office of Naval Research.
† Now with Nuclear Development Associates, Inc., White Plains, New York.
[1] H. Feshbach and V. Weisskopf, Phys. Rev. **76**, 1550 (1949) (henceforth referred to as FW).
[2] Feshbach, Peaslee, and Weisskopf, Phys. Rev. **71**, 145 (1947) (hereafter referred to as FPW).

TABLE I. Cross section for the formation of the compound nucleus by protons. The number in the parentheses is the negative power of 10 by which the tabular entry must be multiplied to obtain the cross section in barns. The nuclear radius was taken to be $r_0A^{\frac{1}{3}}\times10^{-13}$ cm. The calculations were made with $V_0=20$ Mev. $x$ is the ratio of the proton energy to the Coulomb barrier height $B$ which is given in the last row. $Z$ is the atomic number of the target nucleus.

| $x$ \ $Z$ | 10 | | 20 | | 30 | |
|---|---|---|---|---|---|---|
| | $r_0=1.3$ | $r_0=1.5$ | $r_0=1.3$ | $r_0=1.5$ | $r_0=1.3$ | $r_0=1.5$ |
| 0.2 | 1.02(2) | 7.4(3) | 5.6(4) | 2.4(4) | 4.0(5) | 1.8(5) |
| 0.3 | 4.6(2) | 3.7(2) | 7.6(3) | 4.8(3) | 1.5(3) | 1.06(3) |
| 0.4 | 0.100 | 9.1(2) | 3.1(2) | 2.5(2) | 1.2(2) | 9.6(3) |
| 0.5 | 0.175 | 0.166 | 7.4(2) | 7.6(2) | 3.9(2) | 3.9(2) |
| 0.6 | 0.23 | 0.22 | 0.140 | 0.130 | 9.2(2) | 9.0(2) |
| 0.7 | 0.25 | 0.28 | 0.20 | 0.21 | 0.17 | 0.17 |
| 0.8 | 0.29 | 0.32 | 0.24 | 0.27 | 0.22 | 0.24 |
| 0.9 | 0.31 | 0.36 | 0.29 | 0.35 | 0.29 | 0.34 |
| 1.0 | 0.33 | 0.39 | 0.33 | 0.40 | 0.34 | 0.41 |
| 1.1 | 0.35 | 0.42 | 0.37 | 0.45 | 0.40 | 0.48 |
| 1.2 | 0.37 | 0.45 | 0.41 | 0.49 | 0.44 | 0.55 |
| 1.3 | 0.40 | 0.49 | 0.44 | 0.54 | 0.48 | 0.61 |
| 1.4 | 0.43 | 0.52 | 0.46 | 0.58 | 0.52 | 0.67 |
| 1.5 | 0.45 | 0.56 | 0.49 | 0.63 | 0.55 | 0.72 |
| 1.6 | 0.48 | 0.59 | 0.51 | 0.65 | 0.58 | 0.74 |
| 1.7 | 0.51 | 0.61 | 0.52 | 0.67 | 0.61 | 0.77 |
| 1.8 | 0.54 | 0.64 | 0.54 | 0.68 | 0.63 | 0.78 |
| $B$(Mev) | 4.07 | 3.53 | 6.48 | 5.62 | 8.26 | 7.16 |

| $x$ \ $Z$ | 40 | | 50 | | 60 | |
|---|---|---|---|---|---|---|
| | $r_0=1.3$ | $r_0=1.5$ | $r_0=1.3$ | $r_0=1.5$ | $r_0=1.3$ | $r_0=1.5$ |
| 0.2 | 3.9(6) | 1.5(6) | 5.0(7) | 1.47(7) | 7.5(8) | 2.0(8) |
| 0.3 | 3.5(4) | 2.4(4) | 1.05(4) | 5.7(5) | 3.0(5) | 1.68(5) |
| 0.4 | 5.5(3) | 3.9(3) | 2.4(3) | 1.54(3) | 1.06(3) | 7.0(4) |
| 0.5 | 2.5(2) | 2.1(2) | 1.5(2) | 1.23(2) | 9.1(3) | 7.6(3) |
| 0.6 | 5.7(2) | 6.6(2) | 5.2(2) | 4.8(2) | 3.8(2) | 3.5(2) |
| 0.7 | 0.14 | 0.143 | 0.120 | 0.120 | 9.8(2) | 0.102 |
| 0.8 | 0.21 | 0.23 | 0.195 | 0.21 | 0.183 | 0.21 |
| 0.9 | 0.29 | 0.33 | 0.28 | 0.33 | 0.27 | 0.33 |
| 1.0 | 0.36 | 0.43 | 0.37 | 0.44 | 0.38 | 0.46 |
| 1.1 | 0.42 | 0.52 | 0.45 | 0.55 | 0.47 | 0.58 |
| 1.2 | 0.48 | 0.60 | 0.52 | 0.64 | 0.56 | 0.68 |
| 1.3 | 0.53 | 0.67 | 0.59 | 0.73 | 0.63 | 0.78 |
| 1.4 | 0.57 | 0.74 | 0.65 | 0.81 | 0.70 | 0.87 |
| 1.5 | 0.61 | 0.79 | 0.70 | 0.87 | 0.76 | 0.94 |
| 1.6 | 0.64 | 0.83 | 0.74 | 0.92 | 0.80 | 1.01 |
| 1.7 | 0.67 | 0.87 | 0.77 | 0.97 | 0.84 | 1.07 |
| 1.8 | 0.69 | 0.89 | 0.79 | 1.00 | 0.88 | 1.12 |
| $B$(Mev) | 9.86 | 8.55 | 11.28 | 9.81 | 12.69 | 11.0 |

| $x$ \ $Z$ | 70 | | 80 | | 90 | |
|---|---|---|---|---|---|---|
| | $r_0=1.3$ | $r_0=1.5$ | $r_0=1.3$ | $r_0=1.5$ | $r_0=1.3$ | $r_0=1.5$ |
| 0.2 | 1.03(8) | 2.9(9) | 1.66(9) | 3.8(10) | 3.1(10) | 5.9(11) |
| 0.3 | 9.2(6) | 5.3(6) | 3.0(6) | 1.40(6) | 1.08(6) | 4.5(7) |
| 0.4 | 4.8(4) | 3.2(4) | 2.4(4) | 1.52(4) | 1.17(4) | 7.6(5) |
| 0.5 | 5.8(3) | 4.7(3) | 3.5(3) | 2.7(3) | 2.1(3) | 1.75(3) |
| 0.6 | 2.9(2) | 2.7(2) | 2.2(2) | 2.1(2) | 1.7(2) | 1.64(2) |
| 0.7 | 8.2(2) | 8.7(2) | 7.1(2) | 7.5(2) | 6.02(2) | 6.5(2) |
| 0.8 | 0.18 | 0.194 | 0.170 | 0.18 | 0.160 | 0.168 |
| 0.9 | 0.27 | 0.32 | 0.27 | 0.32 | 0.28 | 0.32 |
| 1.0 | 0.38 | 0.47 | 0.40 | 0.48 | 0.41 | 0.49 |
| 1.1 | 0.50 | 0.61 | 0.51 | 0.63 | 0.53 | 0.65 |
| 1.2 | 0.59 | 0.71 | 0.62 | 0.76 | 0.64 | 0.79 |
| 1.3 | 0.67 | 0.84 | 0.71 | 0.88 | 0.75 | 0.93 |
| 1.4 | 0.75 | 0.92 | 0.80 | 0.99 | 0.84 | 1.05 |
| 1.5 | 0.82 | 1.01 | 0.87 | 1.10 | 0.91 | 1.18 |
| 1.6 | 0.87 | 1.10 | 0.94 | 1.20 | 0.99 | 1.28 |
| 1.7 | 0.92 | 1.17 | 0.99 | 1.28 | 1.05 | 1.38 |
| 1.8 | 0.96 | 1.23 | 1.04 | 1.34 | 1.11 | 1.45 |
| $B$(Mev) | 13.9 | 12.1 | 15.2 | 13.1 | 16.2 | 14.1 |

TABLE II. Cross section for the formation of the compound nucleus by deuterons. The number in parentheses is the negative power of 10 by which the tabular entry must be multiplied to obtain the cross section in barns. The interaction distance was taken to be $(r_0A^{\frac{1}{3}}+1.21)10^{-13}$ cm. The calculations were made with $V_0=10$ Mev. $x$ is the ratio of the deuteron energy to the Coulomb barrier height $B$ given in the last row. $Z$ is the atomic number of the target nucleus.

| $x$ \ $Z$ | 10 | | 20 | | 30 | |
|---|---|---|---|---|---|---|
| | $r_0=1.3$ | $r_0=1.5$ | $r_0=1.3$ | $r_0=1.5$ | $r_0=1.3$ | $r_0=1.5$ |
| 0.2 | 4.4(4) | 2.9(4) | 4.7(6) | 2.7(6) | 1.3(7) | 4.6(8) |
| 0.3 | 6.6(3) | 4.5(3) | 4.7(4) | 3.1(4) | 3.7(5) | 2.5(5) |
| 0.4 | 3.0(2) | 2.6(2) | 5.6(3) | 4.5(3) | 1.2(3) | 9.6(4) |
| 0.5 | 7.8(2) | 8.5(2) | 2.4(2) | 2.6(2) | 9.2(3) | 1.0(2) |
| 0.6 | 0.140 | 0.16 | 6.5(2) | 8.2(2) | 3.6(2) | 4.5(2) |
| 0.7 | 0.195 | 0.20 | 0.13 | 0.15 | 9.1(2) | 0.10 |
| 0.8 | 0.26 | 0.28 | 0.21 | 0.23 | 0.18 | 0.20 |
| 0.9 | 0.33 | 0.36 | 0.29 | 0.32 | 0.28 | 0.31 |
| 1.0 | 0.39 | 0.42 | 0.36 | 0.42 | 0.37 | 0.41 |
| 1.1 | 0.43 | 0.48 | 0.42 | 0.50 | 0.46 | 0.51 |
| 1.2 | 0.46 | 0.53 | 0.48 | 0.57 | 0.54 | 0.61 |
| 1.3 | 0.50 | 0.57 | 0.53 | 0.63 | 0.61 | 0.69 |
| 1.4 | 0.53 | 0.60 | 0.58 | 0.68 | 0.68 | 0.76 |
| 1.5 | 0.55 | 0.64 | 0.62 | 0.73 | 0.73 | 0.82 |
| 1.6 | 0.58 | 0.67 | 0.65 | 0.79 | 0.78 | 0.89 |
| 1.7 | 0.60 | 0.69 | 0.68 | 0.82 | 0.81 | 0.94 |
| 1.8 | 0.63 | 0.72 | 0.70 | 0.85 | 0.83 | 0.99 |
| $B$(Mev) | 3.04 | 2.81 | 5.11 | 4.54 | 6.72 | 5.96 |

| $x$ \ $Z$ | 40 | | 50 | | 60 | |
|---|---|---|---|---|---|---|
| | $r_0=1.3$ | $r_0=1.5$ | $r_0=1.3$ | $r_0=1.5$ | $r_0=1.3$ | $r_0=1.5$ |
| 0.2 | 3.4(9) | 1.2(9) | 1.5(10) | 3.8(11) | 7.9(12) | 1.7(12) |
| 0.3 | 4.5(6) | 2.7(6) | 7.0(7) | 3.4(7) | 1.2(7) | 5(8) |
| 0.4 | 3.0(4) | 2.4(4) | 9.6(5) | 6.0(5) | 2.6(5) | 1.7(5) |
| 0.5 | 4.5(3) | 4.4(3) | 1.9(3) | 1.7(3) | 9.0(4) | 7.0(4) |
| 0.6 | 2.4(2) | 2.6(2) | 1.5(2) | 1.5(2) | 9.1(3) | 7.8(3) |
| 0.7 | 7.0(2) | 8.0(2) | 5.4(2) | 5.8(2) | 4.1(2) | 4.4(2) |
| 0.8 | 0.153 | 0.173 | 0.138 | 0.154 | 0.125 | 0.139 |
| 0.9 | 0.26 | 0.29 | 0.25 | 0.29 | 0.25 | 0.28 |
| 1.0 | 0.38 | 0.43 | 0.38 | 0.43 | 0.38 | 0.44 |
| 1.1 | 0.47 | 0.54 | 0.49 | 0.57 | 0.50 | 0.60 |
| 1.2 | 0.56 | 0.65 | 0.59 | 0.69 | 0.62 | 0.75 |
| 1.3 | 0.64 | 0.75 | 0.69 | 0.81 | 0.72 | 0.88 |
| 1.4 | 0.72 | 0.85 | 0.78 | 0.92 | 0.82 | 1.00 |
| 1.5 | 0.79 | 0.91 | 0.86 | 1.01 | 0.91 | 1.11 |
| 1.6 | 0.85 | 0.99 | 0.93 | 1.11 | 0.99 | 1.21 |
| 1.7 | 0.90 | 1.06 | 0.99 | 1.20 | 1.06 | 1.31 |
| 1.8 | 0.94 | 1.13 | 1.03 | 1.27 | 1.11 | 1.39 |
| $B$(Mev) | 8.18 | 7.24 | 9.53 | 8.41 | 10.8 | 9.52 |

| $x$ \ $Z$ | 70 | | 80 | | 90 | |
|---|---|---|---|---|---|---|
| | $r_0=1.3$ | $r_0=1.5$ | $r_0=1.3$ | $r_0=1.5$ | $r_0=1.3$ | $r_0=1.5$ |
| 0.2 | 4(13) | 7(14) | 2(14) | 4(15) | 2(15) | 3(16) |
| 0.3 | 2(8) | 8(9) | 4(9) | 1(9) | 9(10) | 3(10) |
| 0.4 | 1.0(5) | 5.0(6) | 3(6) | 1.9(6) | 1.1(6) | 6.6(7) |
| 0.5 | 4.2(4) | 3.0(4) | 2.1(4) | 1.5(4) | 1.05(4) | 7.2(5) |
| 0.6 | 5.9(3) | 5.2(3) | 3.6(3) | 3.5(3) | 2.5(3) | 2.1(3) |
| 0.7 | 3.4(2) | 3.4(2) | 2.7(2) | 2.5(2) | 2.2(2) | 1.9(2) |
| 0.8 | 0.106 | 0.120 | 0.100 | 0.108 | 9.0(2) | 9.6(2) |
| 0.9 | 0.24 | 0.26 | 0.23 | 0.26 | 0.22 | 0.25 |
| 1.0 | 0.38 | 0.45 | 0.38 | 0.46 | 0.38 | 0.46 |
| 1.1 | 0.52 | 0.62 | 0.53 | 0.65 | 0.55 | 0.67 |
| 1.2 | 0.65 | 0.79 | 0.67 | 0.84 | 0.70 | 0.88 |
| 1.3 | 0.77 | 0.94 | 0.80 | 1.01 | 0.85 | 1.06 |
| 1.4 | 0.88 | 1.09 | 0.93 | 1.17 | 0.98 | 1.22 |
| 1.5 | 0.98 | 1.20 | 1.04 | 1.31 | 1.10 | 1.39 |
| 1.6 | 1.08 | 1.31 | 1.14 | 1.44 | 1.21 | 1.53 |
| 1.7 | 1.15 | 1.42 | 1.23 | 1.54 | 1.30 | 1.63 |
| 1.8 | 1.21 | 1.51 | 1.30 | 1.64 | 1.37 | 1.73 |
| $B$(Mev) | 12.0 | 10.6 | 13.1 | 11.5 | 14.1 | 12.4 |

TABLE III. Cross section for the formation of the compound nucleus by $\alpha$-particles. The number in the parentheses is the negative power of 10 by which the tabular entry must be multiplied to obtain the cross section in barns. The interaction distance was taken to be $(r_0A^{\frac{1}{3}}+1.21)10^{-13}$ cm. The calculations were made with $V_0=5$ Mev. $x$ is the ratio of the alpha-particle energy to the Coulomb barrier height $B$ given in the last row. $Z$ is the atomic number of the target nucleus.

| $x$ \ $Z$ | 10 | | 20 | | 30 | | 50 | 70 | 90 |
|---|---|---|---|---|---|---|---|---|---|
| | $r_0=1.3$ | $r_0=1.5$ | $r_0=1.3$ | $r_0=1.5$ | $r_0=1.3$ | $r_0=1.5$ | $r_0=1.3$ | $r_0=1.3$ | $r_0=1.3$ |
| 0.2 | 7(7) | 8(8) | 2(11) | 3(12) | 5(15) | 8(16) | 9.3(21) | 5.4(26) | 2.88(30) |
| 0.3 | 3.8(5) | 1.6(5) | 1.1(7) | 5(7) | 1(9) | 4(9) | 3.06(13) | 1.80(16) | 4.3(19) |
| 0.4 | 8.4(4) | 5.2(4) | 1.9(5) | 2.3(5) | 1.2(6) | 5.3(7) | 5.7(9) | 5.0(11) | 9.7(13) |
| 0.5 | 7.0(3) | 5.5(3) | 6.8(4) | 5.1(4) | 1.4(4) | 6.0(5) | 2.80(6) | 1.65(7) | 1.15(8) |
| 0.6 | 2.7(2) | 2.5(2) | 6.2(3) | 5.4(3) | 2.3(3) | 1.7(3) | | | |
| 0.7 | 6.1(2) | 6.4(2) | 2.5(2) | 2.7(2) | 1.3(2) | 1.4(2) | | | |
| 0.8 | 0.133 | 0.122 | 7.5(2) | 8.1(2) | 5.0(2) | 5.8(2) | | | |
| 0.9 | 0.166 | 0.19 | 0.145 | 0.167 | 0.136 | 0.158 | | | |
| 1.0 | 0.22 | 0.26 | 0.22 | 0.25 | 0.22 | 0.26 | | | |
| 1.1 | 0.27 | 0.32 | 0.28 | 0.33 | 0.30 | 0.36 | | | |
| 1.2 | 0.31 | 0.37 | 0.34 | 0.40 | 0.37 | 0.46 | | | |
| 1.3 | 0.35 | 0.42 | 0.39 | 0.47 | 0.44 | 0.55 | | | |
| 1.4 | 0.38 | 0.46 | 0.44 | 0.53 | 0.51 | 0.63 | | | |
| 1.5 | 0.41 | 0.50 | 0.48 | 0.59 | 0.56 | 0.70 | | | |
| 1.6 | 0.44 | 0.53 | 0.53 | 0.64 | 0.62 | 0.76 | | | |
| 1.7 | 0.46 | 0.55 | 0.56 | 0.69 | 0.66 | 0.82 | | | |
| 1.8 | 0.47 | 0.57 | 0.59 | 0.73 | 0.70 | 0.86 | | | |
| $B$(Mev) | 6.1 | 5.6 | 10.2 | 9.1 | 13.4 | 11.9 | 19.1 | 24.0 | 28.2 |

nuclear volume. This formula differs from that given in reference 2 by not including the binding energy contribution, which we now feel is best considered as a potential energy.[3] It is convenient to define an energy $V_0$ related to $K_0$ by the expression

$$V_0=\hbar^2K_0^2/2M.$$

From the expression for $K_0$ we find that appropriate values of $V_0$ for protons, deuterons, and alpha-particles are 20, 10, and 5 Mev, respectively.

The radius $R$ is defined as that value of the coordinate $r$ for which the wave number changes from $K$ to $k$. Actually, this change occurs gradually over a distance of the order $1/K$. Hence, the nuclear radius as determined below may differ from values obtained by other means by a much as 1 or 2 times $10^{-13}$ cm.

The cross section that we calculate below is the cross section for the formation of the compound nucleus $\sigma_c$. This quantity is not the same as the reaction cross section $\sigma_r$ defined in FW as the total cross section minus the elastic scattering cross section. $\sigma_c$ exceeds $\sigma_r$ by the magnitude of the capture elastic scattering cross section. The decay of the compound nucleus by emission of the incident particle in such a manner as to leave the residual nucleus in the same quantum state as the target nucleus is referred to as capture elastic scattering.

One of the basic assumptions of the theory is that the probability of capture elastic scattering is very small. That is, the cross section for capture elastic scattering is far exceeded by the sum of the cross sections for other processes such as gamma-ray emission, neutron emission, and inelastic scattering. This restricts the theory to the middle energy region from about 1 Mev above the threshold for neutron emission to about 50 Mev where the interaction of the bombarding particle with other nucleons is no longer so strong and there is evidence[4] that the nucleus is "transparent" in the sense that a particle can pass through it substantially unchanged.

[3] It differs from the formula for $K_0^2$ given in reference 2 also because of an obvious misprint.

## 2. RESULTS

The results of the calculation of $\sigma_c$, the cross section for formation of the compound nucleus, by protons,

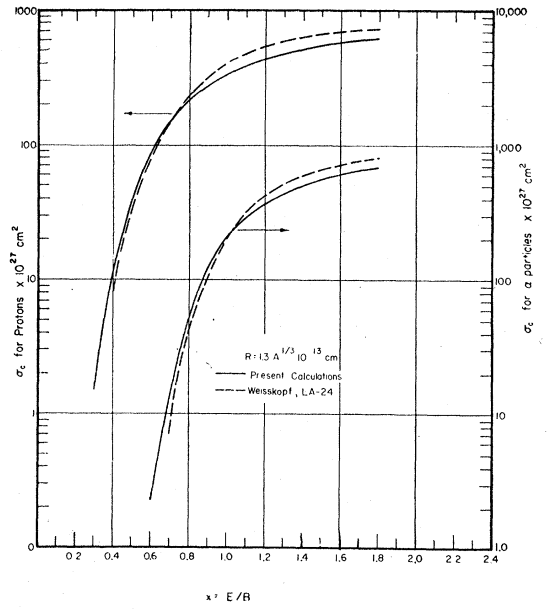


FIG. 1. A comparison of the results of V. Weisskopf [Lecture Series in Nuclear Physics, Report MDDC 1175, 1947 (unpublished)] with the present calculations for the formation of the compound nucleus by proton and alpha-particle bombardment of Zn.

[4] Fernbach, Serber, and Taylor, Phys. Rev. **75**, 1352 (1949).

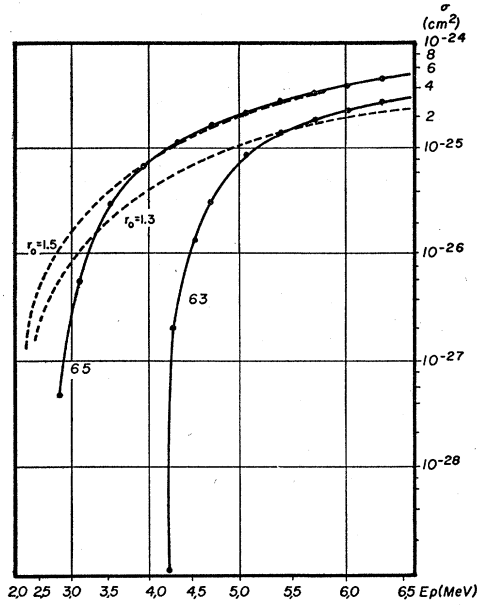


FIG. 2. $Cu^{63}(p,n)Zn^{63}$ and $Cu^{65}(p,n)Zn^{65}$ cross sections. The circles are experimental data from reference 9; the dashed curves are theoretical results for nuclear radii of $r_0A^{\frac{1}{3}}\times10^{-13}$ cm.

deuterons, and alpha-particles are shown in Tables I, II, and III for atomic numbers 10, 20, $\cdots$, 90 when the incident particles are protons and deuterons, and atomic numbers 10, 20, 30, 50, 70, 90 for alpha-particles. The tables cover a variation in energy of the incident particle from 0.2 to 1.8 times the Coulomb barrier height, except in the case of alpha-particle bombardment of nuclei with nuclear charges 50, 70, and 90 where the cross sections are given only for energies up to one-half the Coulomb barrier height.

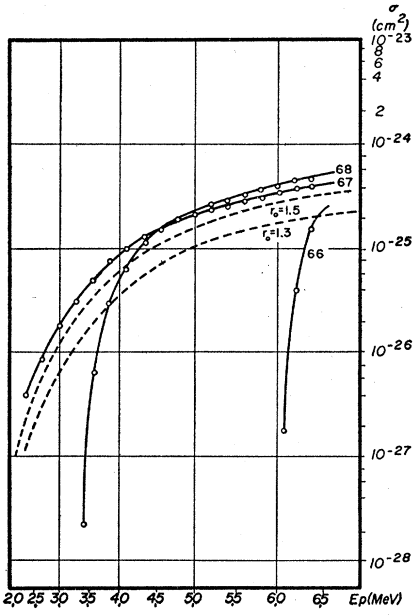


FIG. 3. $Zn^{66}(p,n)Ga^{66}$, $Zn^{67}(p,n)Ga^{67}$, and $Zn^{68}(p,n)Ga^{68}$ cross sections. The circles are experimental points from reference 9; the dashed curves are theoretical results for nuclear radii of $r_0A^{\frac{1}{3}}\times10^{-13}$ cm.

Table I was computed using a nuclear potential, $V_0$ (see part 1 of this paper), of 20 Mev. In Table II $V_0=10$ Mev, while a value of 5 Mev was used in Table III.

The energy is expressed in units of the Coulomb barrier height by means of the dimensionless quantity

$$x=\frac{\epsilon}{B}=\frac{\epsilon}{Zze^2/R},$$

where $Z$ and $z$ are the atomic numbers of the target nucleus and incident particles. The last row of tabular entries are the Coulomb barrier heights.

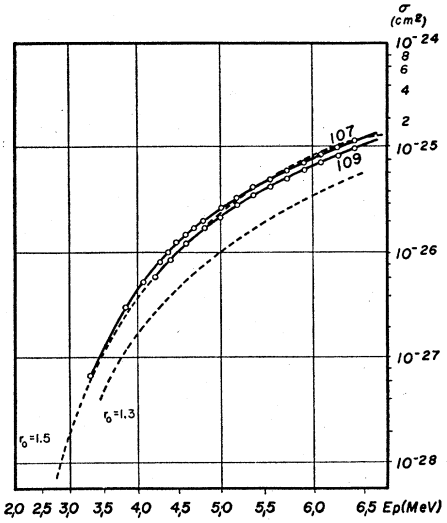


FIG. 4. $Ag^{107}(p,n)Cd^{107}$ and $Ag^{109}(p,n)Cd^{109}$ cross sections. The circles are experimental points from reference 9; the dashed curves are theoretical results for nuclear radii of $r_0A^{\frac{1}{3}}\times10^{-13}$ cm.

Nuclear radii were computed from the formula

$$R=r_0A^{\frac{1}{3}}\times10^{-13}\text{ cm},$$

when the incident particle was a proton, and

$$R=(r_0A^{\frac{1}{3}}+1.21)10^{-13}\text{ cm},$$

when it was either a deuteron or alpha-particle. $A$ is the mass number of the target nucleus. In each table cross sections are given for two values of $r_0$.

Section 5 of this article contains a table from which one can obtain the cross section for formation of the compound nucleus by a charged particle, according to the schematic theory, for a wide range of nuclear radii and nuclear potentials. The table can be applied when the incident particle is a proton or deuteron if the atomic number of the target nucleus exceeds 10. The table yields values for alpha-particles for $Z$ less than 30. The energy range covered is again from 0.2 to 1.8 times the Coulomb barrier height.

A comparison of the present calculations with those reported by Weisskopf[5] for the Zn nucleus is shown in Fig. 1. It will be noted that Weisskopf's cross sections increase more rapidly with energy. In the worst case shown they are 30 percent too small at the lowest energy and 17 percent too large at the highest energy shown in Fig. 1.

It is also interesting to compare the present calculations at energies exceeding the Coulomb barrier height with an approximation that can be found in a semiclassical fashion. We expect $\sigma_c$ to approach $\pi R^2$ for high energies. However, this asymptotic value is attained only for very high energies. For lower energies we proceed as follows. We assume that every particle which strikes the nuclear surface contributes to $\sigma_c$ (sticking probability equal to unity). Then the cross

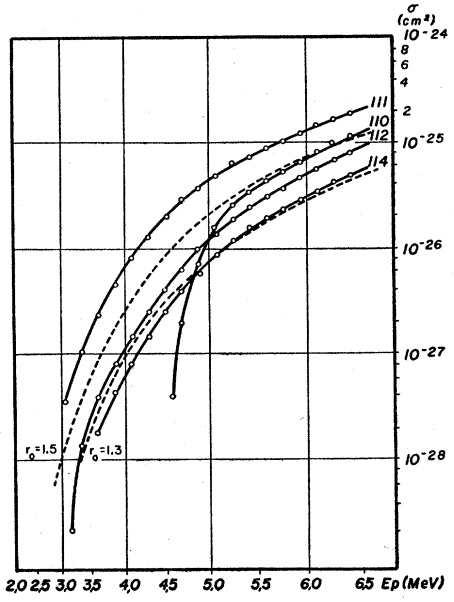


FIG. 5. $Cd^{111}(p,n)In^{111}$, $Cd^{110}(p,n)In^{110}$, $Cd^{112}(p,n)In^{112}$, and $Cd^{114}(p,n)In^{114}$ cross sections. The circles are experimental points from reference 9; the dashed curves are theoretical results for nuclear radii of $r_0A^{\frac{1}{3}}\times10^{-13}$ cm.

section for formation of the compound nucleus is simply $\pi p^2$, where $p$ is the largest impact parameter for which the charged particles encounter the nuclear surface. As in reference 1, we take as the effective nuclear radius $R+\lambda\!\!\!^{-}$. $\lambda\!\!\!^{-}$ is the reduced wavelength of the incident particle and can be considered as its effective radius. A simple calculation in electrodynamics yields

$$\sigma_c=\pi p^2=\pi(R+\lambda\!\!\!^{-})^2\left\{1-\frac{Zze^2/(R+\lambda\!\!\!^{-})}{\epsilon}\right\}.$$

This asymptotic value agrees surprisingly well with the more accurate calculations; the difference being about 15 percent when $x=1.2$ and less for higher values of $x$.

[5] V. Weisskopf, MDDC 1175, 1947 (unpublished).

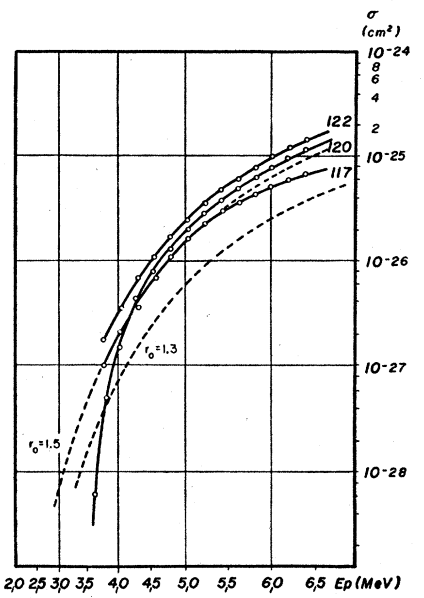


FIG. 6. $Sn^{117}(p,n)Sb^{117}$, $Sn^{120}(p,n)Sb^{120}$, $Sn^{122}(p,n)$ $Sb^{122}$ cross sections. The circles are experimental points from reference 9; the dashed curves are theoretical results for nuclear radii of $r_0A^{\frac{1}{3}}\times10^{-13}$ cm.

An examination of the results shows that cross sections increase with increasing values of the nuclear radius and decreasing values of $V_0$. The shape of the curve for $\sigma_c$ *vs* $E$ is relatively insensitive to $V_0$ in the

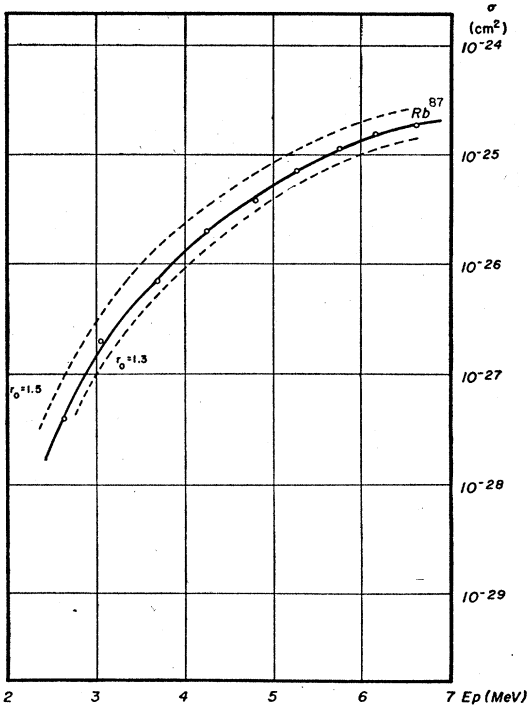


FIG. 7. $Rb^{87}(p,n)Sr^{87}$ cross section. The circles are experimental points from reference 10; the dashed curves are theoretical results for nuclear radii of $r_0A^{\frac{1}{3}}\times10^{-13}$ cm.

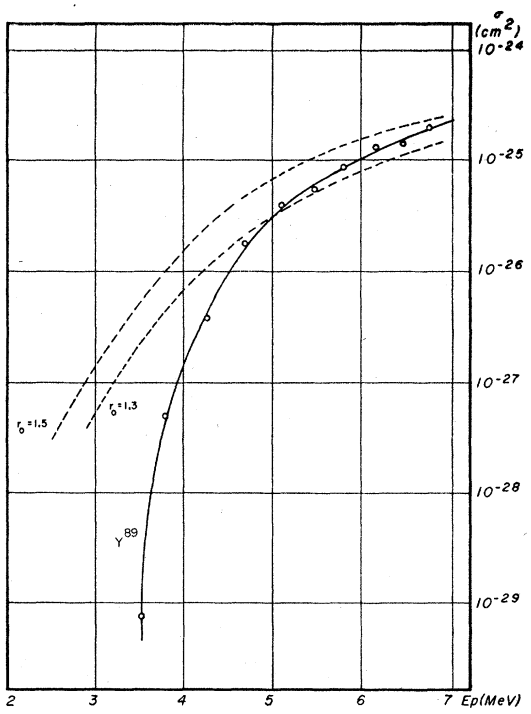


FIG. 8. $Y^{89}(p,n)Zr^{89}$ cross section. The circles are experimental points from reference 10; the dashed curves are theoretical results for nuclear radii of $r_0A^{\frac{1}{3}}\times10^{-13}$ cm.

energy range from 0.3 to 1.0 times the Coulomb barrier height.

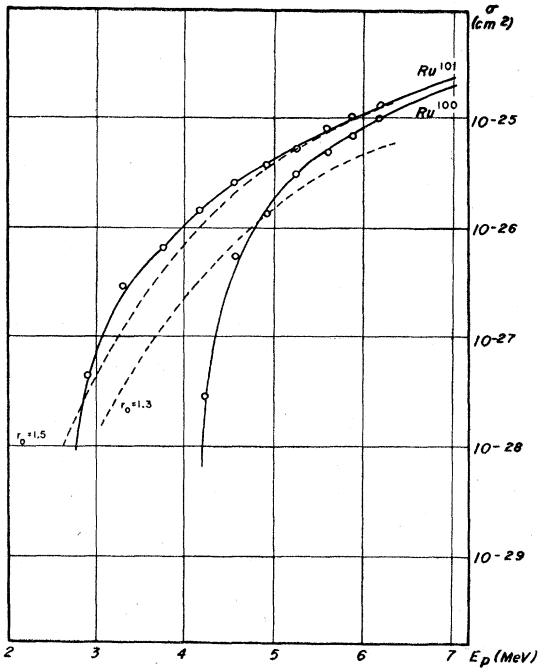


FIG. 9. $Ru^{100}(p,n)Rh^{100}$ and $Ru^{101}(p,n)Rh^{101}$ cross sections. The circles are experimental points from reference 10; the dashed curves are theoretical results for nuclear radii of $r_0A^{\frac{1}{3}}\times10^{-13}$ cm.

### 3. CALCULATION OF THE CROSS SECTION FOR FORMATION OF THE COMPOUND NUCLEUS

The derivation of the results follows that of FW and is based upon the same assumptions.

(a) The energy of the incident charged particle must be high enough so that it is energetically possible for the compound nucleus to decay into many channels; that is, the residual nucleus may be left in many different excited states. Thus, the region of validity includes energies $\epsilon$ which are greater than the first excitation energy of the compound nucleus.

Not only must we assume that it is energetically possible for the compound nucleus to decay into

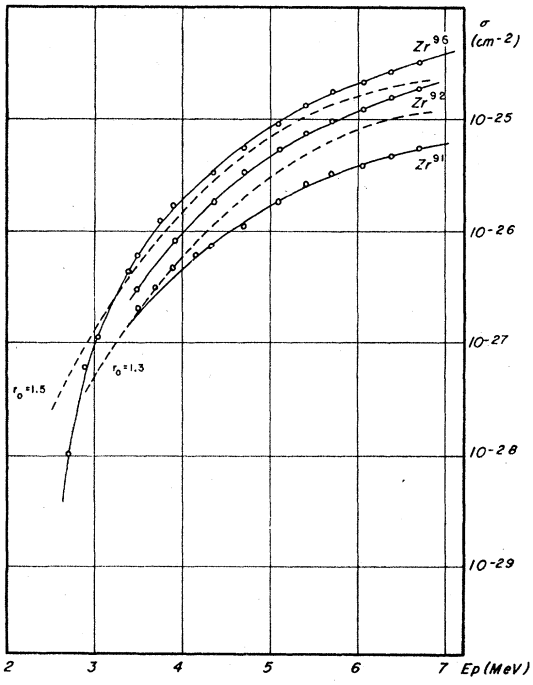


FIG. 10. $Zr^{91}(p,n)Mb^{91}$, $Zr^{92}(p,n)Mb^{92}$, $Zr^{96}(p,n)Mb^{96}$ cross sections. The circles are experimental points from reference 10; the dashed curves are theoretical results for nuclear radii of $r_0A^{\frac{1}{3}}\times10^{-13}$ cm.

channels other than the entrance channel, but we must also postulate:

(b) The interaction between the incoming particle and the nucleons of the target nucleus must be strong enough so that the probability of decay into other channels is high.

Statement (a) defines the low energy limit of the theory, and statement (b) sets the upper energy limit.

If the above conditions are satisfied, then within the nuclear surface the wave function $\psi$ can be represented by a converging wave only.[1] This is mathematically expressed by the boundary condition

$$\frac{d}{dr}\log(r\psi)\,|_{r=R}=-iK,$$

where $K$ is the wave number of the incident particle inside the nucleus. The derivation proceeds exactly as in FW and, in fact, their final result for the reaction cross section, which we repeat here, is valid for charged particles if we define the functions $v_l$, which in FW took account of the centrifugal potential, to now take into account the Coulomb potential also:

$$\sigma_c{}^{(l)}=\frac{4\pi(2l+1)}{k^2}\frac{kK}{k^2|v_l'|^2_{r=R}+K^2|v_l|^2_{r=R}+2kK}.$$

$v_l$ is now the spherical coordinate $r$ times the outgoing radial part of the wave function and is asymptotically

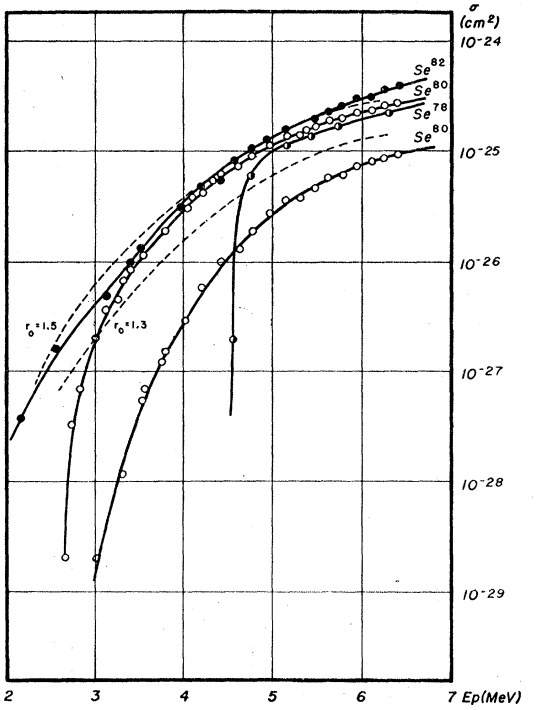


FIG. 11. $Se^{78}(p,n)Br^{78}$, $Se^{80}(p,n)Br^{80}$ (18 min), $Se^{80}(p,n)Br^{80}$ (4.7 hr), and $Se^{82}(p,n)Br^{82}$ cross sections. The cross section for the formation of the 18.5 minute isomer of $Br^{80}$ is the larger of the two shown. The circles are experimental points from reference 10; the dashed curves are theoretical results for nuclear radii of $r_0A^{\frac{1}{3}}\times10^{-13}$ cm.

defined by

$$v_l\underset{a.s}{\longrightarrow}\exp[i\{kr-\alpha\log 2kr-l\pi/2+\delta_l{}^c\}],$$

where

$$\alpha=mZze^2/\hbar^2k$$

and

$$\delta_l{}^c=\arg\Gamma(l+1+i\alpha),$$

with $\Gamma(z)$ being the gamma-function of argument $z$. As before, $k$ is the wave number of the incident particle in the center-of-mass system. $v_l'$ is the derivative of $v_l$ with respect to $kr$.

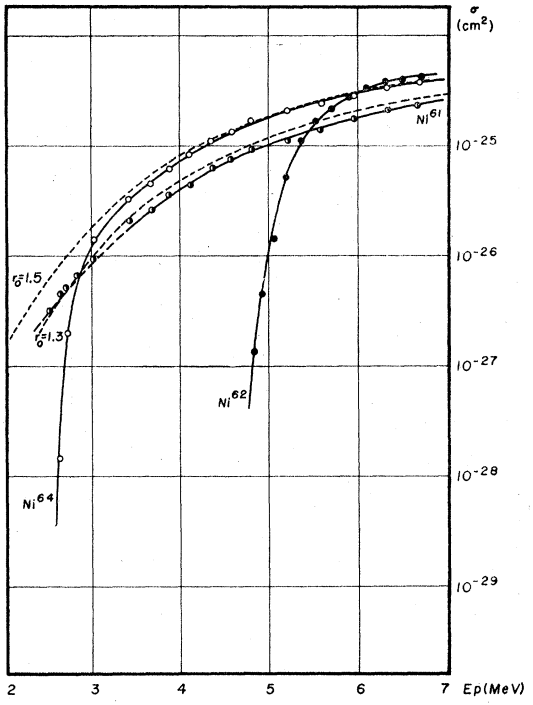


FIG. 12. $Ni^{61}(p,n)Cu^{61}$, $Ni^{62}(p,n)Cu^{62}$, and $Ni^{64}(p,n)Cu^{62}$ cross sections. The circles are experimental points from reference 10; the dashed curves are theoretical results for nuclear radii of $r_0A^{\frac{1}{3}}\times10^{-13}$ cm.

Because the WKB method of solution is not valid near the turning point of the equation for the radial

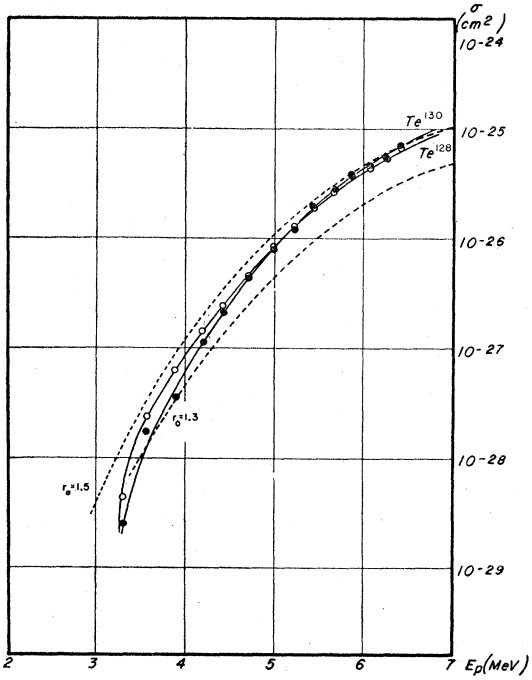


FIG. 13. $Te^{128}(p,n)I^{128}$ and $Te^{130}(p,n)I^{130}$ cross sections. The circles are experimental points from reference 10; the dashed curves are theoretical results for nuclear radii of $r_0A^{\frac{1}{3}}\times10^{-13}$ cm.

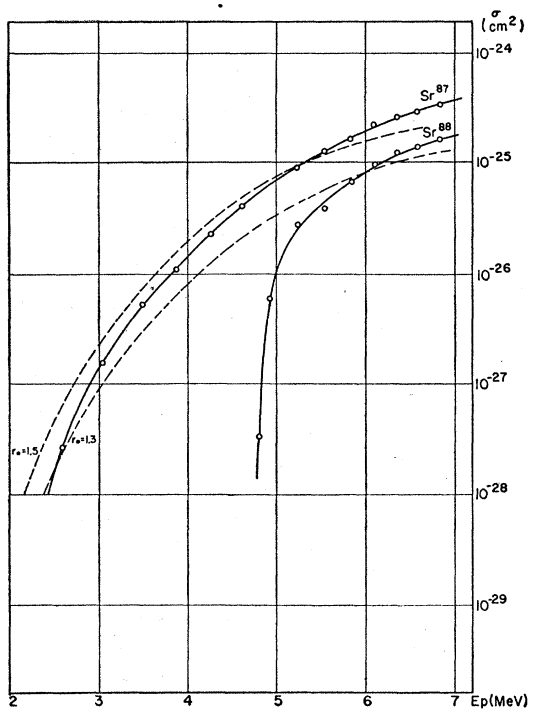


FIG. 14. $Sr^{87}(p,n)Y^{87}$ and $Sr^{88}(p,n)Y^{88}$ cross sections. The circles are experimental points from reference 10; the dashed curves are theoretical results for nuclear radii of $r_0A^{\frac{1}{3}}\times10^{-13}$ cm.

part of the wave function and because the contribution to $\sigma_c$ from angular momenta near the turning point is

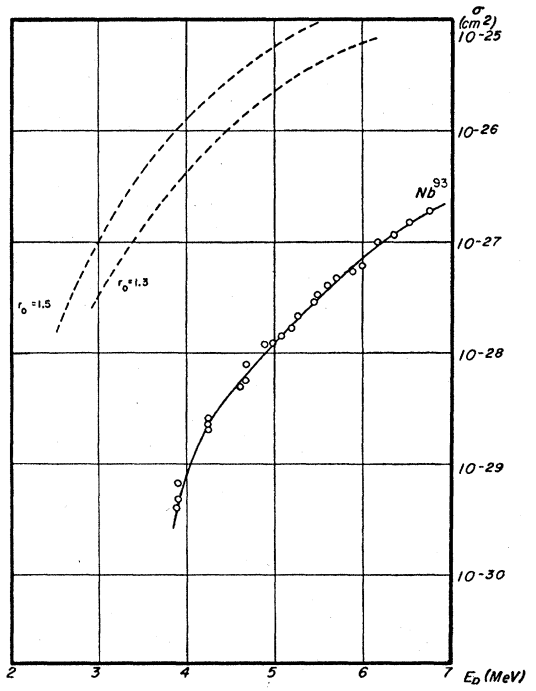


FIG. 15. $Nb^{93}(p,n)Mo^{93}$ cross section. The circles are experimental points from reference 10; the dashed curves are theoretical results for nuclear radii of $r_0A^{\frac{1}{3}}\times10^{-13}$ cm.

appreciable, a more accurate method due to Tyson[6] was used to obtain the functions $v_l$ and $v_l'$. $v_0$ and $v_0'$ were computed accurately and the functions of order one to six were obtained from recursion formulas. For $l>6$ a one-term asymptotic formula not valid near the turning point was employed. The functions $v_l$ are related to Whittaker's function $W_{km}(z)$,[7] so that when the turning point occurred for $l>6$ and the one-term formula could not be used, we employed the more accurate asymptotic expansion given in reference 7.

## 4. COMPARISON WITH EXPERIMENTAL DATA

In this section we shall compare the calculated cross section for the formation of compound nucleus $\sigma_c$

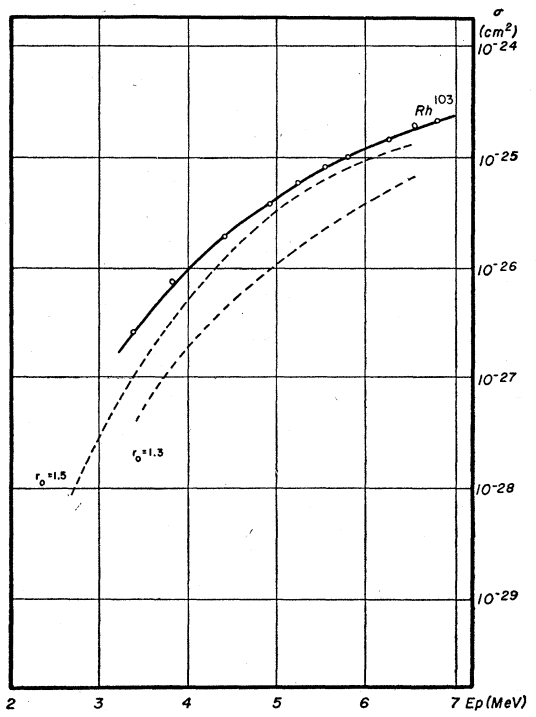


FIG. 16. $Rh^{103}(p,n)Pd^{103}$ cross section. The circles are experimental points from reference 10; the dashed curves are theoretical results for nuclear radii of $r_0A^{\frac{1}{3}}\times10^{-13}$ cm.

with some experimental measurements of $(p,n)$ and $(\alpha;n,2n,\cdots)$ cross sections. Agreement is to be expected when the two conditions set forth in part 3 of this paper are met and when the cross section for neutron emission is a good measure of $\sigma_c$. The assumption that it is energetically possible for the compound nucleus to decay into many channels does not obtain at energies less than about 1 Mev above the threshold for neutron emission. Here the probability for capture elastic scattering is large and the logarithmic derivative of the wave function does not satisfy the boundary condition

[6] J. K. Tyson, Massachusetts Institute of Technology thesis, 1948 (unpublished).

[7] E. T. Whittaker and G. N. Watson, *A Course of Modern Analysis* (MacMillan Company, New York, 1943), Chap. 16.

assumed to hold at the nuclear surface. The cross section for neutron emission is not a good measure of $\sigma_c$ in two energy regions. In the vicinity of the threshold for neutron emission capture elastic scattering and gamma-ray emission will be the favored modes of decay of the compound nucleus, while at energies well above the Coulomb barrier height $(p,p)$ or $(\alpha,\alpha)$ processes can compete favorably with the corresponding neutron emitting processes, especially if neutron emission leads to residual nuclei with a smaller level density. Thus $\sigma_c$

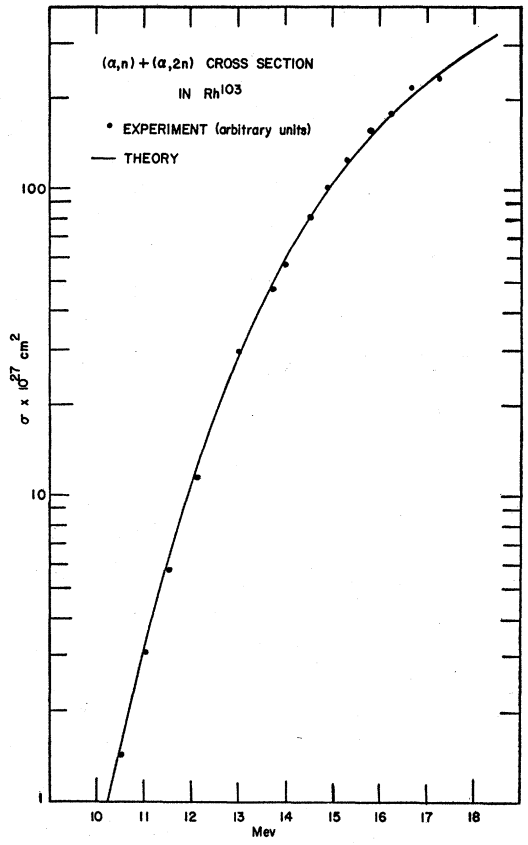


FIG. 17. The sum of the $Rh^{103}(\alpha,n)Ag^{106}$ and $Rh^{103}(\alpha,2n)Ag^{105}$ cross sections. The circles are experimental points from reference 11; the solid curve the theoretical cross section for a nuclear radius of $1.3A^{\frac{1}{3}}\times10^{-13}$ cm. An absolute cross section measurement was not made; the data were normalized for the best fit with the theory.

expected to agree with the $(p,n)$ or $(\alpha;n,2n,\cdots)$ cross sections in a middle energy region extending from about 1 Mev above the threshold for neutron emission to several Mev above the Coulomb barrier height.[8] Outside this region $\sigma_c$ is expected to exceed the $(p,n)$ or $(\alpha;n,2n,\cdots)$ cross section.

[8] Near the threshold for neutron emission where only a few levels of the residual nucleus are involved, consideration of the angular momentum and parity of the nuclear levels and of the emitted particle is necessary. See, for example, H. Feshbach and W. Hauser, Phys. Rev. 87, 366 (1952).

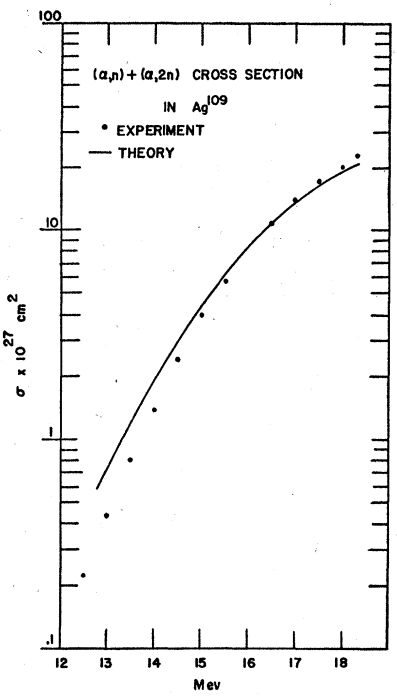


FIG. 18. The sum of the $Ag^{109}(\alpha,n)In^{112}$ and $Ag^{109}(\alpha,2n)In^{111}$ cross sections. The circles are experimental points from reference 11; the solid curve the theoretical result with a nuclear radius of $1.3A^{\frac{1}{3}}\times10^{-13}$ cm.

## A. Proton Reactions

Quantitative investigations of the $(p,n)$ reactions have been carried out at Zürich and reported in the

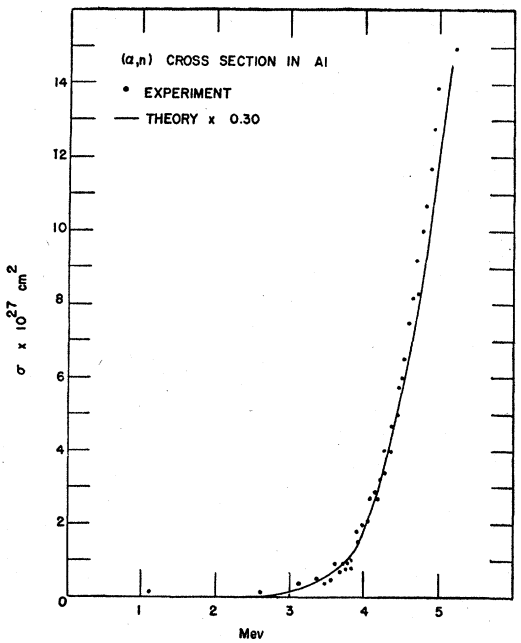


FIG. 19. $Al(\alpha,n)P$ cross section. The circles are experimental points from reference 12. The solid curve is proportional to the theoretical result for a nuclear radius of $1.3A^{\frac{1}{3}}\times10^{-13}$ cm.

TABLE IV. The tabulated quantities are $\log_{10}(\sigma_c/\pi\lambda^2)$, where $\sigma_c$ is the cross section for the formation of the compound nucleus and $\lambda$ is the reduced wavelength $(\lambda/2\pi)$ of the incident particle. The bar over the characteristic indicates that it is negative. All mantissas are positive. For the definitions of $g$, $x$, $V_0$, and $B$, see the text, Sec. 5.

$g=2$

| $x$ \ $V_0/B$ | 1.0 | 2.0 | 3.0 | 4.0 | 5.0 | 6.0 |
|---|---|---|---|---|---|---|
| 0.2 | $\bar{3}.772$ | $\bar{3}.725$ | $\bar{3}.672$ | $\bar{3}.625$ | $\bar{3}.572$ | $\bar{3}.525$ |
| 0.3 | $\bar{2}.625$ | $\bar{2}.770$ | $\bar{2}.729$ | $\bar{2}.675$ | $\bar{2}.635$ | $\bar{2}.600$ |
| 0.4 | $\bar{1}.275$ | $\bar{1}.360$ | $\bar{1}.319$ | $\bar{1}.280$ | $\bar{1}.218$ | $\bar{1}.190$ |
| 0.5 | $\bar{1}.731$ | $\bar{1}.659$ | $\bar{1}.605$ | $\bar{1}.563$ | $\bar{1}.527$ | $\bar{1}.496$ |
| 0.6 | 0.0358 | $\bar{1}.974$ | $\bar{1}.926$ | $\bar{1}.887$ | $\bar{1}.854$ | $\bar{1}.826$ |
| 0.7 | 0.220 | 0.165 | 0.120 | 0.0829 | 0.0537 | 0.0243 |
| 0.8 | 0.3619 | 0.309 | 0.267 | 0.233 | 0.203 | 0.177 |
| 0.9 | 0.466 | 0.417 | 0.378 | 0.345 | 0.316 | 0.291 |
| 1.0 | 0.547 | 0.497 | 0.464 | 0.433 | 0.405 | 0.381 |
| 1.1 | 0.623 | 0.580 | 0.544 | 0.514 | 0.489 | 0.464 |
| 1.2 | 0.689 | 0.649 | 0.615 | 0.587 | 0.562 | 0.540 |
| 1.3 | 0.743 | 0.705 | 0.672 | 0.647 | 0.623 | 0.602 |
| 1.4 | 0.789 | 0.754 | 0.724 | 0.698 | 0.675 | 0.654 |
| 1.5 | 0.829 | 0.796 | 0.767 | 0.743 | 0.721 | 0.701 |
| 1.6 | 0.866 | 0.834 | 0.807 | 0.783 | 0.762 | 0.743 |
| 1.7 | 0.902 | 0.872 | 0.846 | 0.824 | 0.803 | 0.785 |
| 1.8 | 0.936 | 0.907 | 0.883 | 0.861 | 0.841 | 0.823 |

$g=3$

| $x$ \ $V_0/B$ | 1.0 | 2.0 | 3.0 | 4.0 |
|---|---|---|---|---|
| 0.2 | $\bar{4}.36$ | $\bar{4}.33$ | $\bar{4}.30$ | $\bar{4}.28$ |
| 0.3 | $\bar{2}.06$ | $\bar{2}.00$ | $\bar{3}.97$ | $\bar{3}.94$ |
| 0.4 | $\bar{1}.00$ | $\bar{2}.94$ | $\bar{2}.88$ | $\bar{2}.84$ |
| 0.5 | $\bar{1}.58$ | $\bar{1}.52$ | $\bar{1}.48$ | $\bar{1}.43$ |
| 0.6 | $\bar{1}.97$ | $\bar{1}.90$ | $\bar{1}.85$ | $\bar{1}.81$ |
| 0.7 | 0.242 | 0.175 | 0.126 | 0.090 |
| 0.8 | 0.358 | 0.374 | 0.329 | 0.290 |
| 0.9 | 0.575 | 0.525 | 0.482 | 0.447 |
| 1.0 | 0.694 | 0.646 | 0.606 | 0.573 |
| 1.1 | 0.784 | 0.738 | 0.704 | 0.672 |
| 1.2 | 0.867 | 0.822 | 0.785 | 0.756 |
| 1.3 | 0.925 | 0.886 | 0.854 | 0.829 |
| 1.4 | 0.989 | 0.954 | 0.924 | 0.893 |
| 1.5 | 1.037 | 1.000 | 0.974 | 0.946 |
| 1.6 | 1.083 | 1.045 | 1.021 | 0.995 |
| 1.7 | 1.128 | 1.096 | 1.070 | 1.046 |
| 1.8 | 1.155 | 1.124 | 1.103 | 1.075 |

$g=4$

| $x$ \ $V_0/B$ | 1.0 | 1.6 | 1.8 | 2.0 | 3.0 | 4.0 |
|---|---|---|---|---|---|---|
| 0.2 | $\bar{5}.21$ | $\bar{5}.11$ | $\bar{5}.10$ | $\bar{5}.09$ | $\bar{5}.05$ | $\bar{5}.00$ |
| 0.3 | $\bar{3}.36$ | $\bar{3}.30$ | $\bar{3}.29$ | $\bar{3}.29$ | $\bar{3}.24$ | $\bar{3}.20$ |
| 0.4 | $\bar{2}.59$ | $\bar{2}.52$ | $\bar{2}.51$ | $\bar{2}.50$ | $\bar{2}.45$ | $\bar{2}.41$ |
| 0.5 | $\bar{1}.34$ | $\bar{1}.28$ | $\bar{1}.28$ | $\bar{1}.27$ | $\bar{1}.23$ | $\bar{1}.18$ |
| 0.6 | $\bar{1}.869$ | $\bar{1}.820$ | $\bar{1}.800$ | $\bar{1}.793$ | $\bar{1}.738$ | $\bar{1}.702$ |
| 0.7 | 0.230 | 0.185 | 0.174 | 0.160 | 0.108 | 0.069 |
| 0.8 | 0.484 | 0.442 | 0.431 | 0.420 | 0.372 | 0.330 |
| 0.9 | 0.658 | 0.623 | 0.614 | 0.605 | 0.560 | 0.520 |
| 1.0 | 0.802 | 0.770 | 0.760 | 0.750 | 0.710 | 0.675 |
| 1.1 | 0.906 | 0.878 | 0.869 | 0.862 | 0.830 | 0.793 |
| 1.2 | 1.000 | 0.975 | 0.966 | 0.959 | 0.920 | 0.888 |
| 1.3 | 1.080 | 1.051 | 1.042 | 1.035 | 0.998 | 0.968 |
| 1.4 | 1.148 | 1.124 | 1.115 | 1.108 | 1.073 | 1.042 |
| 1.5 | 1.201 | 1.179 | 1.172 | 1.166 | 1.133 | 1.103 |
| 1.6 | 1.254 | 1.232 | 1.225 | 1.216 | 1.187 | 1.162 |
| 1.7 | 1.298 | 1.278 | 1.270 | 1.262 | 1.235 | 1.210 |
| 1.8 | 1.327 | 1.310 | 1.303 | 1.297 | 1.272 | 1.245 |

$g=5$

| $x$ \ $V_0/B$ | 0.6 | 0.8 | 1.0 | 1.5 | 2.0 | 3.0 |
|---|---|---|---|---|---|---|
| 0.2 | $\bar{7}.90$ | $\bar{7}.89$ | $\bar{7}.87$ | $\bar{7}.80$ | $\bar{7}.77$ | $\bar{7}.70$ |
| 0.3 | $\bar{4}.585$ | $\bar{4}.550$ | $\bar{4}.540$ | $\bar{4}.525$ | $\bar{4}.510$ | $\bar{4}.460$ |
| 0.4 | $\bar{2}.130$ | $\bar{2}.105$ | $\bar{2}.095$ | $\bar{2}.060$ | $\bar{2}.040$ | $\bar{3}.985$ |
| 0.5 | $\bar{1}.115$ | $\bar{1}.095$ | $\bar{1}.075$ | $\bar{1}.045$ | $\bar{1}.014$ | $\bar{2}.962$ |
| 0.6 | $\bar{1}.778$ | $\bar{1}.760$ | $\bar{1}.744$ | $\bar{1}.704$ | $\bar{1}.665$ | $\bar{1}.612$ |
| 0.7 | 0.231 | 0.217 | 0.196 | 0.159 | 0.125 | 0.070 |
| 0.8 | 0.540 | 0.525 | 0.504 | 0.468 | 0.440 | 0.394 |
| 0.9 | 0.756 | 0.742 | 0.724 | 0.692 | 0.663 | 0.616 |
| 1.0 | 0.921 | 0.904 | 0.889 | 0.858 | 0.831 | 0.788 |
| 1.1 | 1.038 | 1.027 | 1.018 | 0.987 | 0.966 | 0.926 |
| 1.2 | 1.142 | 1.131 | 1.118 | 1.093 | 1.067 | 1.030 |
| 1.3 | 1.230 | 1.216 | 1.210 | 1.183 | 1.159 | 1.117 |
| 1.4 | 1.302 | 1.291 | 1.280 | 1.258 | 1.234 | 1.200 |
| 1.5 | 1.360 | 1.347 | 1.342 | 1.319 | 1.298 | 1.267 |
| 1.6 | 1.411 | 1.401 | 1.392 | 1.371 | 1.354 | 1.323 |
| 1.7 | 1.450 | 1.444 | 1.436 | 1.416 | 1.397 | 1.369 |
| 1.8 | 1.485 | 1.481 | 1.472 | 1.456 | 1.443 | 1.420 |

$g=6$

| $x$ \ $V_0/B$ | 0.6 | 0.8 | 1.0 | 1.5 | 2.0 |
|---|---|---|---|---|---|
| 0.2 | $\bar{8}.61$ | $\bar{8}.60$ | $\bar{8}.59$ | $\bar{8}.58$ | $\bar{8}.58$ |
| 0.3 | $\bar{5}.83$ | $\bar{5}.82$ | $\bar{5}.80$ | $\bar{5}.78$ | $\bar{5}.77$ |
| 0.4 | $\bar{3}.650$ | $\bar{3}.640$ | $\bar{3}.620$ | $\bar{3}.595$ | $\bar{3}.565$ |
| 0.5 | $\bar{2}.841$ | $\bar{2}.827$ | $\bar{2}.815$ | $\bar{2}.778$ | $\bar{2}.748$ |
| 0.6 | $\bar{1}.644$ | $\bar{1}.622$ | $\bar{1}.605$ | $\bar{1}.564$ | $\bar{1}.525$ |
| 0.7 | 0.183 | 0.164 | 0.146 | 0.108 | 0.075 |
| 0.8 | 0.551 | 0.533 | 0.514 | 0.476 | 0.448 |
| 0.9 | 0.808 | 0.791 | 0.774 | 0.737 | 0.709 |
| 1.0 | 0.994 | 0.978 | 0.964 | 0.932 | 0.902 |
| 1.1 | 1.135 | 1.123 | 1.108 | 1.077 | 1.048 |
| 1.2 | 1.242 | 1.228 | 1.216 | 1.190 | 1.164 |
| 1.3 | 1.330 | 1.316 | 1.306 | 1.281 | 1.260 |
| 1.4 | 1.409 | 1.398 | 1.390 | 1.368 | 1.344 |
| 1.5 | 1.472 | 1.462 | 1.454 | 1.432 | 1.410 |
| 1.6 | 1.525 | 1.515 | 1.505 | 1.484 | 1.469 |
| 1.7 | 1.574 | 1.565 | 1.557 | 1.537 | 1.518 |
| 1.8 | 1.615 | 1.606 | 1.598 | 1.582 | 1.566 |

$g=7$

| $x$ \ $V_0/B$ | 0.4 | 0.6 | 0.8 | 1.0 | 1.5 | 2.0 |
|---|---|---|---|---|---|---|
| 0.2 | $\bar{9}.25$ | $\bar{9}.25$ | $\bar{9}.25$ | $\bar{9}.24$ | $\bar{9}.23$ | $\bar{9}.23$ |
| 0.3 | $\bar{5}.04$ | $\bar{5}.03$ | $\bar{5}.02$ | $\bar{5}.01$ | $\bar{5}.00$ | $\bar{6}.98$ |
| 0.4 | $\bar{3}.19$ | $\bar{3}.17$ | $\bar{3}.16$ | $\bar{3}.15$ | $\bar{3}.12$ | $\bar{3}.09$ |
| 0.5 | $\bar{2}.565$ | $\bar{2}.555$ | $\bar{2}.540$ | $\bar{2}.520$ | $\bar{2}.490$ | $\bar{2}.465$ |
| 0.6 | $\bar{1}.513$ | $\bar{1}.492$ | $\bar{1}.471$ | $\bar{1}.452$ | $\bar{1}.411$ | $\bar{1}.382$ |
| 0.7 | 0.150 | 0.124 | 0.104 | 0.086 | 0.046 | 0.015 |
| 0.8 | 0.577 | 0.556 | 0.535 | 0.520 | 0.482 | 0.449 |
| 0.9 | 0.868 | 0.847 | 0.834 | 0.812 | 0.775 | 0.746 |
| 1.0 | 1.075 | 1.056 | 1.039 | 1.024 | 0.990 | 0.661 |
| 1.1 | 1.225 | 1.212 | 1.197 | 1.183 | 1.153 | 1.122 |
| 1.2 | 1.340 | 1.326 | 1.310 | 1.300 | 1.274 | 1.246 |
| 1.3 | 1.429 | 1.419 | 1.404 | 1.394 | 1.367 | 1.346 |
| 1.4 | 1.516 | 1.503 | 1.494 | 1.483 | 1.458 | 1.438 |
| 1.5 | 1.576 | 1.567 | 1.557 | 1.548 | 1.525 | 1.509 |
| 1.6 | 1.636 | 1.628 | 1.618 | 1.608 | 1.589 | 1.568 |
| 1.7 | 1.693 | 1.683 | 1.672 | 1.664 | 1.642 | 1.623 |
| 1.8 | 1.735 | 1.728 | 1.719 | 1.704 | 1.695 | 1.677 |

TABLE IV.—*Continued.*

| $x$ \ $V_0/B$ | 0.4 | 0.6 | 0.8 | 1.0 | 1.5 |
|---|---|---|---|---|---|
| | | | $g=8$ | | |
| 0.2 | $\bar{1}1.98$ | $\bar{1}1.98$ | $\bar{1}1.98$ | $\bar{1}1.97$ | $\bar{1}1.95$ |
| 0.3 | $\bar{6}.25$ | $\bar{6}.25$ | $\bar{6}.24$ | $\bar{6}.23$ | $\bar{6}.22$ |
| 0.4 | $\bar{4}.715$ | $\bar{4}.700$ | $\bar{4}.685$ | $\bar{4}.670$ | $\bar{4}.620$ |
| 0.5 | $\bar{2}.275$ | $\bar{2}.255$ | $\bar{2}.245$ | $\bar{2}.225$ | $\bar{2}.195$ |
| 0.6 | $\bar{1}.346$ | $\bar{1}.326$ | $\bar{1}.308$ | $\bar{1}.290$ | $\bar{1}.250$ |
| 0.7 | 0.082 | 0.056 | 0.036 | 0.017 | 1.980 |
| 0.8 | 0.575 | 0.554 | 0.533 | 0.515 | 0.480 |
| 0.9 | 0.900 | 0.880 | 0.861 | 0.846 | 0.807 |
| 1.0 | 1.127 | 1.108 | 1.091 | 1.076 | 1.042 |
| 1.1 | 1.292 | 1.276 | 1.260 | 1.242 | 1.215 |
| 1.2 | 1.413 | 1.398 | 1.384 | 1.374 | 1.346 |
| 1.3 | 1.510 | 1.496 | 1.482 | 1.474 | 1.446 |
| 1.4 | 1.597 | 1.585 | 1.574 | 1.564 | 1.542 |
| 1.5 | 1.661 | 1.652 | 1.643 | 1.634 | 1.615 |
| 1.6 | 1.733 | 1.723 | 1.710 | 1.702 | 1.678 |
| 1.7 | 1.784 | 1.773 | 1.762 | 1.752 | 1.734 |
| 1.8 | 1.834 | 1.825 | 1.815 | 1.807 | 1.788 |

| $x$ \ $V_0/B$ | 0.2 | 0.4 | 0.6 | 0.8 | 1.0 | 1.2 |
|---|---|---|---|---|---|---|
| | | | $g=9$ | | | |
| 0.2 | $\bar{1}2.68$ | $\bar{1}2.68$ | $\bar{1}2.68$ | $\bar{1}2.68$ | $\bar{1}2.68$ | $\bar{1}2.68$ |
| 0.3 | $\bar{7}.47$ | $\bar{7}.47$ | $\bar{7}.46$ | $\bar{7}.45$ | $\bar{7}.44$ | $\bar{7}.43$ |
| 0.4 | $\bar{4}.22$ | $\bar{4}.21$ | $\bar{4}.20$ | $\bar{4}.18$ | $\bar{4}.16$ | $\bar{4}.15$ |
| 0.5 | $\bar{3}.986$ | $\bar{3}.968$ | $\bar{3}.952$ | $\bar{3}.940$ | $\bar{3}.925$ | $\bar{3}.910$ |
| 0.6 | $\bar{1}.200$ | $\bar{1}.170$ | $\bar{1}.152$ | $\bar{1}.136$ | $\bar{1}.122$ | $\bar{1}.108$ |
| 0.7 | 0.027 | 0.007 | $\bar{1}.983$ | $\bar{1}.962$ | $\bar{1}.944$ | $\bar{1}.926$ |
| 0.8 | 0.590 | 0.565 | 0.545 | 0.524 | 0.504 | 0.486 |
| 0.9 | 0.952 | 0.928 | 0.908 | 0.889 | 0.874 | 0.758 |
| 1.0 | 1.196 | 1.175 | 1.155 | 1.138 | 1.125 | 1.006 |
| 1.1 | 1.366 | 1.348 | 1.334 | 1.318 | 1.304 | 1.218 |
| 1.2 | 1.500 | 1.481 | 1.465 | 1.451 | 1.439 | 1.388 |
| 1.3 | 1.598 | 1.584 | 1.571 | 1.558 | 1.548 | 1.538 |
| 1.4 | 1.686 | 1.674 | 1.661 | 1.651 | 1.640 | 1.630 |
| 1.5 | 1.754 | 1.740 | 1.730 | 1.717 | 1.708 | 1.697 |
| 1.6 | 1.835 | 1.822 | 1.806 | 1.795 | 1.788 | 1.775 |
| 1.7 | 1.876 | 1.866 | 1.856 | 1.846 | 1.838 | 1.827 |
| 1.8 | 1.925 | 1.915 | 1.906 | 1.896 | 1.889 | 1.877 |

| $x$ \ $V_0/B$ | 0.2 | 0.4 | 0.6 | 0.8 | 1.0 |
|---|---|---|---|---|---|
| | | | $g=10$ | | |
| 0.2 | $\bar{1}3.35$ | $\bar{1}3.35$ | $\bar{1}3.35$ | $\bar{1}3.35$ | $\bar{1}3.35$ |
| 0.3 | $\bar{8}.658$ | $\bar{8}.656$ | $\bar{8}.655$ | $\bar{8}.653$ | $\bar{8}.652$ |
| 0.4 | $\bar{5}.715$ | $\bar{5}.700$ | $\bar{5}.690$ | $\bar{5}.675$ | $\bar{5}.660$ |
| 0.5 | $\bar{3}.684$ | $\bar{3}.662$ | $\bar{3}.642$ | $\bar{3}.640$ | $\bar{3}.640$ |
| 0.6 | $\bar{1}.024$ | $\bar{2}.996$ | $\bar{2}.977$ | $\bar{2}.958$ | $\bar{2}.944$ |
| 0.7 | $\bar{1}.948$ | $\bar{1}.927$ | $\bar{1}.904$ | $\bar{1}.885$ | $\bar{1}.865$ |
| 0.8 | 0.574 | 0.549 | 0.526 | 0.506 | 0.487 |
| 0.9 | 0.976 | 0.953 | 0.933 | 0.912 | 0.899 |
| 1.0 | 1.240 | 1.219 | 1.198 | 1.182 | 1.168 |
| 1.1 | 1.422 | 1.404 | 1.388 | 1.373 | 1.360 |
| 1.2 | 1.564 | 1.545 | 1.529 | 1.514 | 1.501 |
| 1.3 | 1.668 | 1.653 | 1.640 | 1.628 | 1.618 |
| 1.4 | 1.757 | 1.745 | 1.731 | 1.723 | 1.712 |
| 1.5 | 1.828 | 1.815 | 1.805 | 1.795 | 1.785 |
| 1.6 | 1.924 | 1.911 | 1.899 | 1.886 | 1.880 |
| 1.7 | 1.957 | 1.942 | 1.933 | 1.924 | 1.915 |
| 1.8 | 2.002 | 1.990 | 1.980 | 1.971 | 1.964 |

| $x$ \ $V_0/B$ | 0.2 | 0.4 | 0.6 | 0.8 | 1.0 |
|---|---|---|---|---|---|
| | | | $g=11$ | | |
| 0.2 | $\bar{1}4.05$ | $\bar{1}4.05$ | $\bar{1}4.05$ | $\bar{1}4.05$ | $\bar{1}4.05$ |
| 0.3 | $\bar{9}.850$ | $\bar{9}.848$ | $\bar{9}.845$ | $\bar{9}.843$ | $\bar{9}.842$ |
| 0.4 | $\bar{5}.210$ | $\bar{5}.202$ | $\bar{5}.190$ | $\bar{5}.180$ | $\bar{5}.168$ |
| 0.5 | $\bar{3}.360$ | $\bar{3}.344$ | $\bar{3}.328$ | $\bar{3}.328$ | $\bar{3}.328$ |
| 0.6 | $\bar{2}.756$ | $\bar{2}.756$ | $\bar{2}.756$ | $\bar{2}.756$ | $\bar{2}.756$ |
| 0.7 | $\bar{1}.865$ | $\bar{1}.844$ | $\bar{1}.822$ | $\bar{1}.803$ | $\bar{1}.785$ |
| 0.8 | 0.556 | 0.535 | 0.510 | 0.487 | 0.465 |
| 0.9 | 0.996 | 0.975 | 0.955 | 0.934 | 0.920 |
| 1.0 | 1.283 | 1.262 | 1.241 | 1.224 | 1.212 |
| 1.1 | 1.474 | 1.456 | 1.439 | 1.425 | 1.412 |
| 1.2 | 1.625 | 1.606 | 1.592 | 1.577 | 1.560 |
| 1.3 | 1.736 | 1.722 | 1.705 | 1.693 | 1.680 |
| 1.4 | 1.828 | 1.815 | 1.800 | 1.791 | 1.784 |
| 1.5 | 1.900 | 1.887 | 1.876 | 1.872 | 1.865 |
| 1.6 | 2.005 | 1.995 | 1.984 | 1.942 | 1.932 |
| 1.7 | 2.027 | 2.014 | 2.004 | 1.996 | 1.990 |
| 1.8 | 2.071 | 2.060 | 2.053 | 2.042 | 2.038 |

literature.[9,10] Unfortunately, the experimental energies do not exceed 7 Mev and comparison with the theory above the Coulomb barrier is not possible.

The experimental data are plotted in Figs. 2–16. In nearly every case a nuclear radius between $1.3A^{\frac{1}{3}}$ and $1.5A^{\frac{1}{3}}$ gives as good a fit as can be obtained, considering the large variation of cross section from isotope to isotope. Two exceptions occur in the cases of Nb and Rh, Figs. 15 and 16, respectively. In the former the theoretical value is too high and in the latter too low.

In several cases measurements were made near the threshold for neutron emission. In every case the large discrepancy between the $(p,n)$ cross section and $\sigma_c$ disappears at about 1 Mev above the threshold.

## B. Alpha-Particle Reactions

Some cross sections for neutron emission following bombardment by alpha-particles have been measured. In Figs. 17 through 21 the experimental values are shown along with the theoretical curve for $\sigma_c$. In applying the schematic theory to calculate $\sigma_c$ for alpha-particles we used an interaction distance of

$$(1.3A^{\frac{1}{3}}+1.21)10^{-13} \text{ cm};$$

$1.21\times10^{-13}$ cm represents the radius of the alpha-particle. A nuclear potential of $-5$ Mev was arbitrarily used in all cases.

Tendam and Bradt[11] have investigated the $(\alpha,n)$ and $(\alpha,2n)$ reactions in rhodium and silver. In Figs. 17 and

[9] Blaser, Boehm, Marmier, and Peaslee, Helv. Phys. Acta **24**, 3 (1951).

[10] Blaser, Boehm, Marmier, and Scherrer, Helv. Phys. Acta **24**. 441 (1951).

[11] D. J. Tendam and H. L. Bradt, Phys. Rev. **72**, 1118 (1947). One of the authors has kindly informed us of an error of a factor of 10 that was made in plotting the results of the Ag$(\alpha;n,2n)$ experiment in this reference.

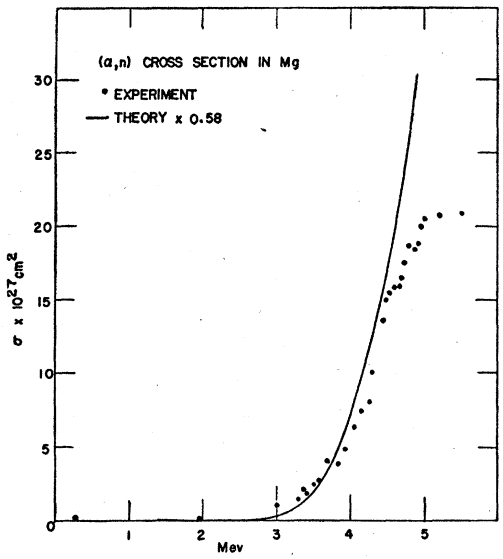


FIG. 20. Mg($\alpha$,$n$)Si cross section. The circles are experimental points from reference (12). The solid curve is proportional to the theoretical result for a nuclear radius of $1.3A^{\frac{1}{3}}\times10^{-13}$ cm.

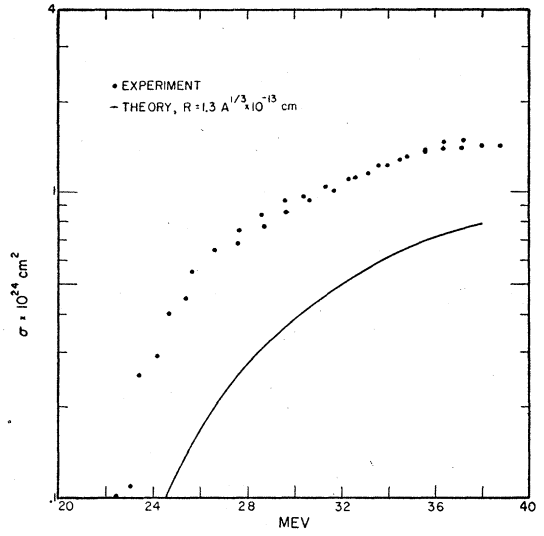


FIG. 21. The sum of the $Bi^{209}(\alpha,2n)At^{211}$ and $Bi^{209}(\alpha,3n)At^{210}$ cross sections. The circles are experimental data from reference 13. The solid curve is the theoretical result for a nuclear radius of $1.3A^{\frac{1}{3}}\times10^{-13}$ cm.

18 we compare the theoretical values of $\sigma_c$ with the sum of these cross sections. Only relative values were measured for rhodium. The agreement is excellent.

Halpern[12] has measured ($\alpha$,$n$) cross sections for Be, Mg, and Al using polonium $\alpha$-particles. Be is certainly too light to be compared with schematic theory results. Mg and Al are light enough so that the validity of the theory is in doubt. However, examination of Figs. 19 and 20 shows that although the theory overestimates the magnitude of the cross section, it does predict the energy dependence of the cross section quite well.

Figure 21 exhibits the theoretical values of $\sigma_c$ and the sum of the ($\alpha$,$2n$) and ($\alpha$,$3n$) cross sections for bismuth as measured by Kelly and Segrè.[13] The calculated cross section has the right energy dependence but too small a magnitude. The use of a larger nuclear radius than that employed here ($7.7\times10^{-13}$ cm) would tend to improve the fit.

## 5. TABLES FOR COMPUTING $\sigma_c$

In this section we tabulate in a more general form than above the information required to predict the cross section for formation of the compound nucleus by proton and deuteron bombardment when the atomic number of the atomic nucleus exceeds 10. The tables yield information about alpha-particle bombardment only for atomic numbers $Z<30$. In every case the energy range is from 0.2 to 1.8 times the Coulomb barrier.

The tabulated values are $\log_{10}(\sigma_c/\pi\lambda\!\!\!^{-2})$, where $\lambda\!\!\!^{-2}=1/k^2=\hbar^2/2m\epsilon$. $\epsilon$ is the kinetic energy of the incident particle in the center-of-mass system, and $m$ is the reduced mass.

The values of $\sigma_c$ are tabulated in terms of the dimensionless quantities $x$ and $g$ which are defined after Bethe as follows:

$$x=\epsilon/B, \quad \text{with} \quad B=Zze^2/R,$$

and

$$g^2=2mZze^2R/\hbar^2.$$

$Z$ and $z$ are the atomic numbers of the target nucleus and bombarding particle, $e$ is the electronic charge, and $R$ is the interaction distance.

A brief description of the method used to obtain the Coulomb wave functions used in preparing the tables given here is given in Sec. 3 of this paper. It is our intention to publish these functions and their derivatives elsewhere.

The wave functions needed for $g=2$ were obtained in part from tables prepared by Bloch *et al.*[14] These joined smoothly onto our calculations for the higher $g$ values.

The author wishes to express his thanks to Professor Feshbach and Professor Weisskopf for their advice during the preparation of this article. Miss Mida Karakashian carried out the numerical computations and her help is gratefully acknowledged. For preparation of the figures the author is indebted to Miss Nina Kropoff and Miss Jane Breckwoldt.

[12] I. Halpern, Phys. Rev. **76**, 248 (1949).
[13] E. L. Kelly and E. Segrè, Phys. Rev. **75**, 999 (1949).
[14] Bloch, Hull, Broyles, Bouricius, Freeman, and Breit, Phys. Rev. **80**, 553 (1950).